Neoplasma 2020; 67(5): 1032–1041

doi:10.4149/neo_2020_191019N1061

Circular RNA circ_0000615 knockdown suppresses the development of nasopharyngeal cancer through regulating the miR-338-3p/FGF2 axis

H.S. LIU[1], R.N. ZHENG[2,*], L.B. GUO[3], X.J. FU[1]

[1]Department of Otolaryngology Head and Neck Surgery, Guangdong Second Provincial General Hospital, Guangzhou, Guangdong, China; [2]Department of Oncology, Affiliated Dongguan People's Hospital, Southern Medical University, Dongguan, Guangdong, China; [3]Department of Oncology, Guangdong Second Provincial General Hospital, Guangzhou, Guangdong, China

**Correspondence: zrn1983@126.com*

Received October 19, 2019 / Accepted January 7, 2020

Nasopharyngeal cancer (NPC) is a type of head and neck cancer with a high rate of metastasis. Circular RNAs (circRNAs) were reported to be related to the development of human cancers. This research aimed to investigate the functional mechanism of circRNA circ_0000615 in NPC. The gene expression was examined by quantitative real-time polymerase chain reaction (qRT-PCR) or western blot. The 3-(4,5-dimethylthiazol-2-yl)-2,5-diphenyltetrazolium bromide (MTT) assay was employed to assess cell proliferation ability. Transwell assay was used to measure cell migratory and invasive abilities. Furthermore, the interaction between miR-338-3p and circ_0000615 or fibroblast growth factor 2 (FGF2) was predicted by starBase v.2.0 and then confirmed by the dual-luciferase reporter assay. Besides, the mouse xenograft experiment was carried out to explore the effect of circ_0000615 on tumor growth in vivo. We detected increased levels of circ_0000615 and FGF2, along with a decreased level of miR-338-3p in NPC tissues and cells. Circ_0000615 knockdown suppressed the proliferation, migration, invasion, and EMT of NPC cells. Interestingly, circ_0000615 interacted with miR-338-3p, and miR-338-3p targeted FGF2. Circ_0000615 inhibited miR-338-3p expression to upregulate the FGF2 level. Furthermore, both miR-338-3p depletion and FGF2 overexpression weakened the effect of circ_0000615 knockdown on NPC cell progression. Besides, circ_0000615 knockdown repressed tumor growth in vivo. In conclusion, our findings demonstrated that circ_0000615 knockdown suppressed the growth of NPC cells via modulating miR-338-3p/FGF2 axis, providing a theoretical basis for the treatment of NPC.

Key words: circ_0000615, miR-338-3p, FGF2, cell growth, nasopharyngeal cancer

Nasopharyngeal cancer (NPC), with a high rate of metastasis, is common cancer in Southern China [1, 2]. After radiotherapy, the 5-year survival rate of NPC patients at stage I and II is approximately 90% [3]. However, many patients with NPC suffer from recurrence as well as metastasis [4]. Moreover, drug resistance becomes a major obstacle for the chemotherapy of NPC [5]. Therefore, it is of urgency to analyze the molecular mechanism of NPC development for the therapy of NPC patients.

In human cancers, a lot of non-coding RNAs, including long non-coding RNAs (lncRNAs) and microRNAs (miRNAs), have shown to act as a group of pivotal regulators [6, 7]. The analysis of circular RNA (circRNA) functional mechanism further enriches the roles of non-coding RNAs in cancers [8]. Present evidence suggests that circRNAs are related to the proliferation, mobility, apoptosis, and epithelial-mesenchymal transition (EMT) of cancer cells [9, 10]. Circ_0000615 (circRNA ZNF609), identified as a circRNA, was reported to regulate NPC cell proliferation and mobility [11]. This result indicated that circ_0000615 exerted a crucial function in NPC development. However, the functional mechanism of circ_0000615 in NPC is less reported.

miRNAs, with around 22 nucleotides, are considered as a family of sponges for messenger RNAs (mRNAs) to induce the degradation or suppress translation of mRNA in human cancers [12]. Furthermore, miRNAs can regulate the levels of diverse mRNAs and mediate a variety of cell progression [13]. Increasing studies suggested that miRNAs were involved in the development of various cancers, such as pancreatic cancer [14], breast cancer [15], colon cancer [16], and NPC [17]. Shan et al. showed that miR-338-3p repressed the proliferation and mobility of NPC cells through modulating the level of hypoxia-induced factor

1α (HIF-1α) [18]. However, whether miR-338-3p affecting NPC development by regulating other genes is unclear.

Fibroblast growth factor 2 (FGF2), identified as a mitogen, is a member of the FGF family that exerts important function in the progression of cell development [19, 20]. In mammals, FGF modulated the growth of cells by interacting with FGF receptors (FGFRs) [21]. Previous evidence suggested that FGF2 acted as an oncogene and was considered as a prognostic marker in NPC [22], meaning that FGF2 was a crucial regulator in NPC development. Therefore, it is essential to explore the role and functional mechanism of FGF2 in NPC.

Here, we determined the levels of circ_0000615, miR-338-3p, FGF2 in NPC tissues and cells, and analyzed the function of circ_0000615 in NPC cells. Furthermore, the roles of miR-338-3p and FGF2 in circ_0000615-regulated cell progression were explored. Besides, we investigated the effect of circ_0000615 on tumor growth *in vivo*.

Materials and methods

Tissues and cell culture. Thirty NPC tissues and 30 adjacent normal tissues were obtained from the patients at the Guangdong Second Provincial General Hospital. Our research was approved by the Ethics Review Committees of Guangdong Second Provincial General Hospital. Informed consent was provided by all patients.

Human normal nasopharyngeal epithelial cells (NP64) and NPC cells (5–8F, 6–10B, HK1, and SUNE1) were purchased from the Cell Bank of the Chinese Academy of Sciences (Shanghai, China). These cells were maintained in Roswell Park Memorial Institute-1640 (RPMI-1640) medium (Thermo Fisher Scientific, Waltham, MA, USA) containing 10% fetal bovine serum (FBS; Hyclone, Logan, UT, USA), 100 IU/ml penicillin (Millipore, Bedford, MA, USA), as well as 100 mg/ml streptomycin (Millipore) at 37 °C with 5% CO_2.

RNA extraction and quantitative real-time polymerase chain reaction (qRT-PCR). Trizol reagent (Invitrogen, Carlsbad, CA, USA) was applied to isolate RNA in line with the recommended protocol. Then, complementary DNA (cDNA) was generated using the Reverse Transcription Kit (TaKaRa, Tokyo, Japan), and qRT-PCR was conducted using SYBR Premix ExTaq kit (TaKaRa). The data were analyzed using the $2^{-\Delta\Delta Ct}$ method. U6 and glyceraldehyde 3-phosphate dehydrogenase (GAPDH) were used as the internal genes. The primers sequence were as follows: circ_0000615 (Forward(F),5'-CAGCGCTCAATCCTTTGGGA-3';Reverse (R), 5'-GACCTGCCACATTGGTCAGTA-3'), miR-338-3p (F, 5'-TTAGTGTACCAGCCAT-3'; R, 5'-GAATGCGGGAGCGAA-3'), FGF2 (F, 5'-GGCTTCTTCCTGCGCATCCA-3'; R, 5'-GCTCTTAGCAGACATTGGAAGA-3'), U6 (F, 5'-TGCGGGTGCTCGCTTCGGCAGC-3'; R, 5'-CCAGTGCAGGGTCCGAGGT-3'), and GAPDH (F, 5'-ATCACTGCCACCCAGAAGAC-3'; R, 5'-TTTCTAGACGGCAGGTCAGG-3').

Subcellular fractionation location. Briefly, the cells were cultured and collected. Then, 200 μl Lysis Buffer J (Life Technologies, Carlsbad, CA) was added for the cell lysis. After centrifugation, the supernatant containing cytoplasmic RNA and the remaining liquid containing nuclear RNA were separated. Next, buffer SK and absolute ethanol were added to the solution, and column centrifugation was used to collect RNA. Finally, cytoplasmic RNA and nuclear RNA were determined using qRT-PCR.

RNase R treatment. 3 U/μg of RNase R (Epicentre Biotechnologies, Madison, WI, USA) was used to treat total RNA (5 μg) for 15 min twice at 37 °C.

Cell transfection. Small interfering RNA against circ_0000615 (si-circ_0000615), small hairpin RNA against circ_0000615 (sh-circ_0000615), miR-338-3p mimic (miR-338-3p), miR-338-3p inhibitor (anti-miR-338-3p), and their negative control (si-NC, sh-NC, miR-NC, and anti-miR-NC) were obtained from GenePharma (Shanghai, China). For the overexpression of FGF2 or circ_0000615, its sequence was inserted into the pcDNA3.1 vector (GenePharma). Lipofectamine 3000 (Invitrogen) was employed to perform the transfection assay.

Cell proliferation assay. The 3-(4,5-dimethylthiazol-2-yl)-2,5-diphenyltetrazolium bromide (MTT) kit (Promega, Madison, WI, USA) was chosen to measure cell proliferation ability according to the user's manual. Briefly, 5–8F or 6–10B cells were transfected and then cultured for 0 h, 24 h, 48 h, or 72 h, respectively. Then, the MTT solution was applied to treat the cells. Subsequently, the product was dissolved using dimethyl sulfoxide (DMSO). Finally, the microplate reader (Bio-Rad, Richmond, CA, USA) was employed to examine the absorbance at 490 nm.

Cell migration and invasion assay. Transwell chamber (BD Biosciences, San Jose, CA, USA) was used to assess cell migratory ability based on the user's manual. Briefly, the top chamber was introduced with 100 μl serum-free medium containing transfected 5–8F or 6–10B cells, and to the bottom chamber, 500 μl medium containing 10% FBS was added. After 12 h culture, the cells on the top chamber were removed. Subsequently, the number of migratory cells was analyzed using the microscope. The same steps were performed for invasion assay when the insert was coated with the Matrigel (BD Biosciences, San Jose, CA, USA).

Western blot assay. Total proteins were obtained from NPC tissues or cells using lysis buffer (Beyotime Biotechnology, Shanghai, China). Subsequently, western blot was performed as described previously [23]. The primary antibodies against E-cadherin (1:1000, ab15148), N-cadherin (1:1000, ab18203), Vimentin (1:1000, ab137321), FGF2 (1:1000, ab126861), and GAPDH (1:1000, ab181602), and corresponding secondary antibodies (1:2000, ab205718) were provided by Abcam (Cambridge, MA, USA) in this study.

The dual-luciferase reporter assay. The interaction between miR-338-3p and circ_0000615 or FGF2 was predicted by starBase v2.0. Wild type circ_0000615 or FGF2

(circ_0000615 WT or FGF2 3'-UTR-WT) or mutant type circ_0000615 or FGF2 (circ_0000615 MUT or FGF2 3'-UTR-MUT) was cloned into the pGL3 vector (Promega). Every construct and miR-NC or miR-338-3p were co-transfected into 5–8F and 6–10B cells. After 48 h culture, the luciferase density was examined using the dual-luciferase assay system (Promega).

Mouse xenografts. 6 weeks old female SCID mice were selected for this experiment that was carried out based on the guidance of the National Animal Care and Ethics Institution and was approved by the Animal Research Committee of Guangdong Second Provincial General Hospital. Briefly, the mice were subcutaneously injected with 5–8F cells transfected with sh-circ_0000615 or sh-NC. After 7 days, tumor volume (length × width^2/2) was calculated every 4 days. After day 27, the tumors were removed and tumor weights were analyzed.

Statistical analysis. The data were analyzed by Student's t-test, and then expressed as the mean ± standard deviation (SD). The relationship of gene levels was evaluated using the analysis of Pearson correlation. A p-value <0.05 was considered statistically significant. Each data group represented 3 biological replicates × 3 technical replicates unless otherwise indicated.

Results

Circ_0000615 expression was upregulated in NPC tissues and cells. Firstly, the qRT-PCR assay was performed to detect the level of circ_0000615 in NPC tissues. The results suggested that circ_0000615 level was significantly higher in NPC tissues than that in adjacent normal tissues (Figure 1A). Moreover, an increased circ_0000615 level was observed in NPC cells (Figure 1B). On the other hand, we analyzed the level of circ_0000615 in nuclei and cytoplasm of NPC cells. As shown in Figures 1C and 1D, circ_0000615 level is lower in the nucleus than that in the cytoplasm. Besides, the stabilization of circ_0000615 structure was investigated through the treatment of RNase R. The results demonstrated that circ_0000615 was stable (Figures 1E, 1F). Therefore, circ_0000615 might act as an oncogene in NPC development.

Circ_0000615 knockdown suppressed NPC cell proliferation, migration, invasion, and EMT. To further investigate the function of circ_0000615, si-circ_0000615 was used to knock down the level of circ_0000615 in 5–8F and 6–10B cells. As shown in Figure 2A, the transfection with si-circ_0000615 dramatically downregulated circ_0000615 expression. Then, the MTT assay was employed to assess cell proliferation ability. The results suggested that circ_0000615 knockdown suppressed cell proliferation in 5–8F and 6–10B cells (Figures 2B, 2C). Moreover, the transwell assay confirmed that cell migratory and invasive abilities were remarkably suppressed by circ_0000615 knockdown (Figures 2D, 2E). Besides, we analyzed the levels of EMT-related proteins, E-cadherin, N-cadherin, and Vimentin, and found that the E-cadherin level was upregulated and the levels of N-cadherin, as well as Vimentin, were downregulated by circ_0000615 knockdown (Figures 2F–2I). These data indicated that circ_0000615 knockdown repressed the growth of NPC cells.

Circ_0000615 was a sponge for miR-338-3p. Online tool starBase v2.0 predicted that miR-338-3p was a poten-

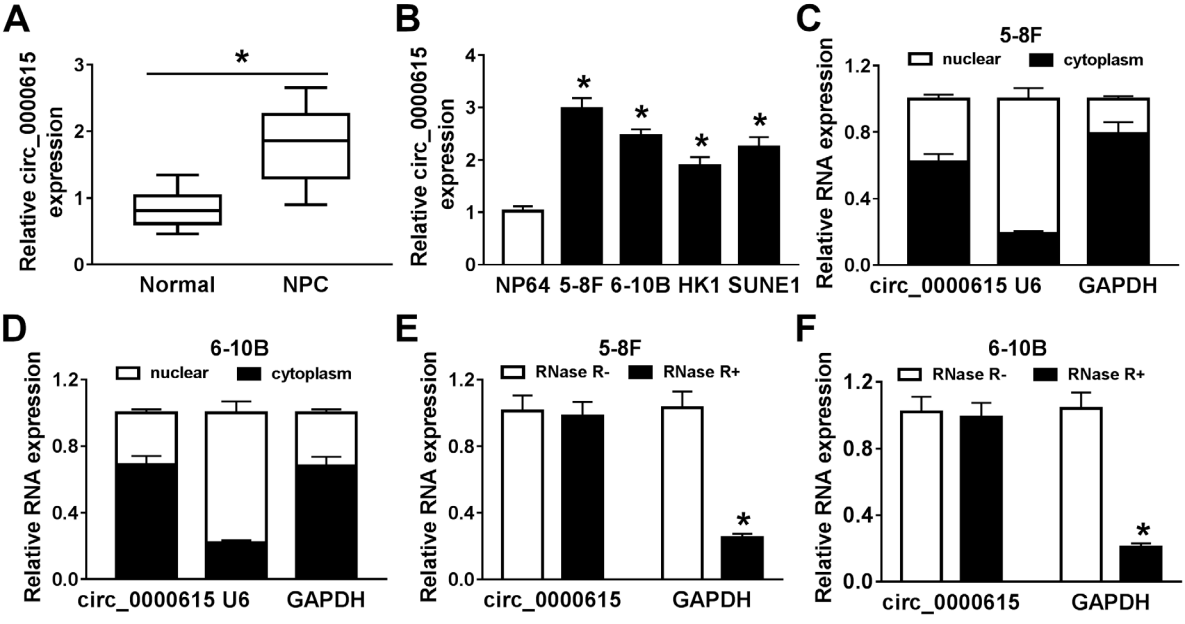

Figure 1. The level of circ_0000615 in NPC tissues and cells. A, B) The expression of circ_0000615 was detected by qRT-PCR assay in NPC and adjacent normal tissues (A) as well as NPC and normal cells (B). C, D) The levels of circ_0000615, U6, and GAPDH were determined in nuclei and cytoplasm of NPC cells. E, F) The levels of circ_0000615 and GAPDH were examined after the treatment of RNase R. *p<0.05

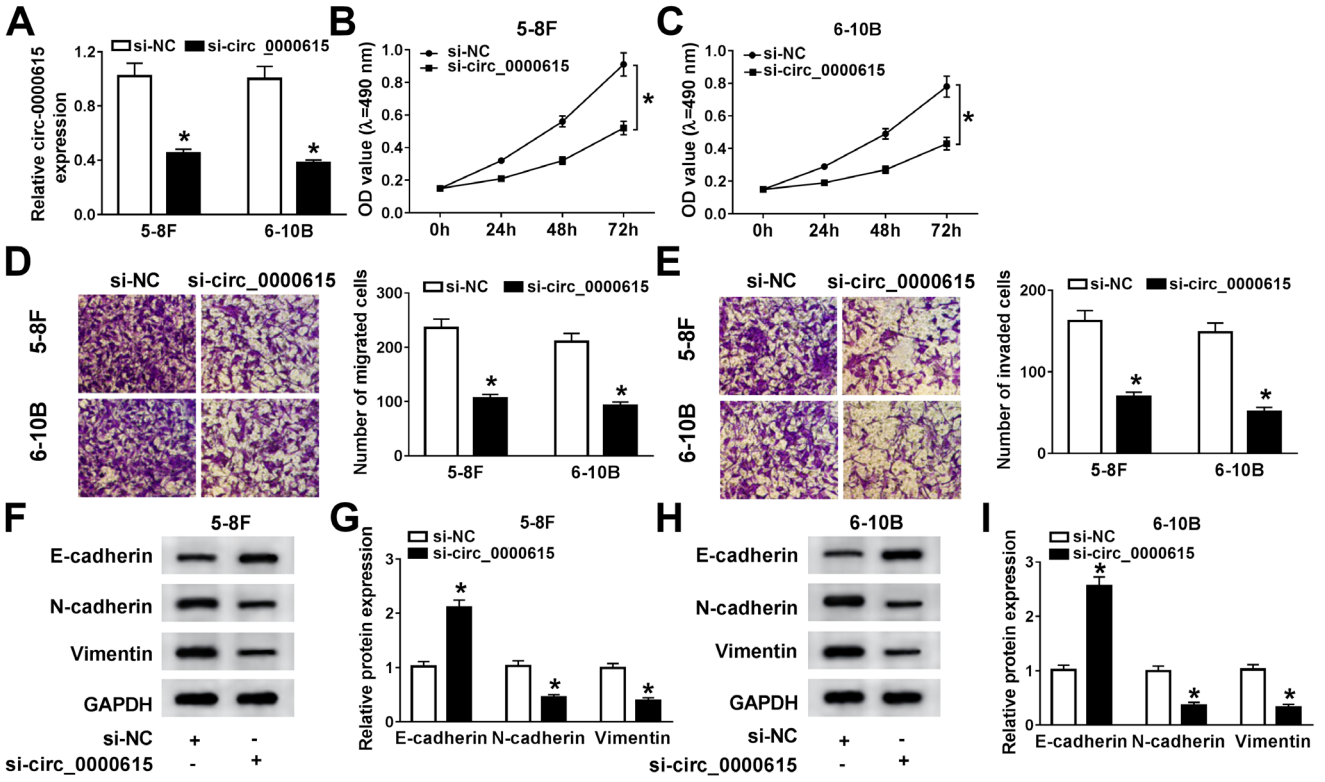

Figure 2. The function of circ_0000615 in NPC cells. A) Circ_0000615 expression was determined in 5–8F and 6–10B cells transfected with si-NC or si-circ_0000615. B, C) The MTT assay was performed to measure cell proliferation ability. D, E) The transwell assay was employed to assess cell migratory and invasive abilities. F–I) The levels of E-cadherin, N-cadherin, and Vimentin were detected by western blot assay. *p<0.05

tial target of circ_0000615 (Figure 3A). Next, the dual-luciferase reporter assay was employed to verify this prediction. As demonstrated in Figures 3B and 3C, miR-338-3p overexpression significantly reduced the luciferase activity of circ_0000615-WT, whereas didn't change the luciferase activity of circ_0000615-MUT, meaning that circ_0000615 interacted with miR-338-3p via the miR-338-3p-binding site. Some circRNAs are capable of regulating the abundance of available miRNAs through sequestering miRNAs [24]. Thus, we further explored whether circ_0000615 affected miR-338-3p expression. The results demonstrated that miR-338-3p expression was upregulated by circ_0000615 knockdown and downregulated by circ_0000615 overexpression (Figure 3D). On the other hand, we determined the level of miR-338-3p and found that miR-338-3p level was remarkably decreased in NPC tissues/cells compared with normal tissues/cells (Figures 3E, 3F). Furthermore, the relationship between circ_0000615 and miR-338-3p was explored. As expected, the miR-338-3p level was negatively correlated with circ_0000615 level in NPC tissues (Figure 3G). All these data suggested that circ_0000615 targeted miR-338-3p and downregulated miR-338-3p abundance.

miR-338-3p knockdown reversed the effect of circ_0000615 depletion on NPC cell progression. To investigate whether circ_0000615 affected NPC cell growth through inhibiting miR-338-3p expression, 5–8F and 6–10B cells were transfected with si-NC, si-circ_0000615, si-circ_0000615 + anti-miR-NC, or si-circ_0000615 + anti-miR-338-3p, respectively. Firstly, the qRT-PCR assay confirmed that miR-338-3p expression was upregulated due to the depletion of circ_0000615, and then downregulated by the transfection with anti-miR-338-3p (Figures 4A, 4B). Next, we analyzed cell proliferation ability using MTT assay and found that circ_0000615 knockdown significantly suppressed cell proliferation, whereas this action was weakened by miR-338-3p depletion (Figures 4C, 4D). Moreover, the transwell assay suggested that cell migratory and invasive abilities were attenuated by circ_0000615 knockdown, and then partly rescued by miR-338-3p depletion (Figures 4E, 4F). Besides, the levels of three EMT markers were determined. As shown in Figures 4G–4J, miR-338-3p depletion reversed the effect of circ_0000615 knockdown on the levels of EMT markers. These data indicated that circ_0000615 repressed miR-338-3p expression to regulate the growth of NPC cells.

miR-338-3p targeted FGF2. Online tool starBase v2.0 predicted that FGF2 was a potential target of miR-338-3p (Figure 5A). Next, we carried out the dual-luciferase reporter

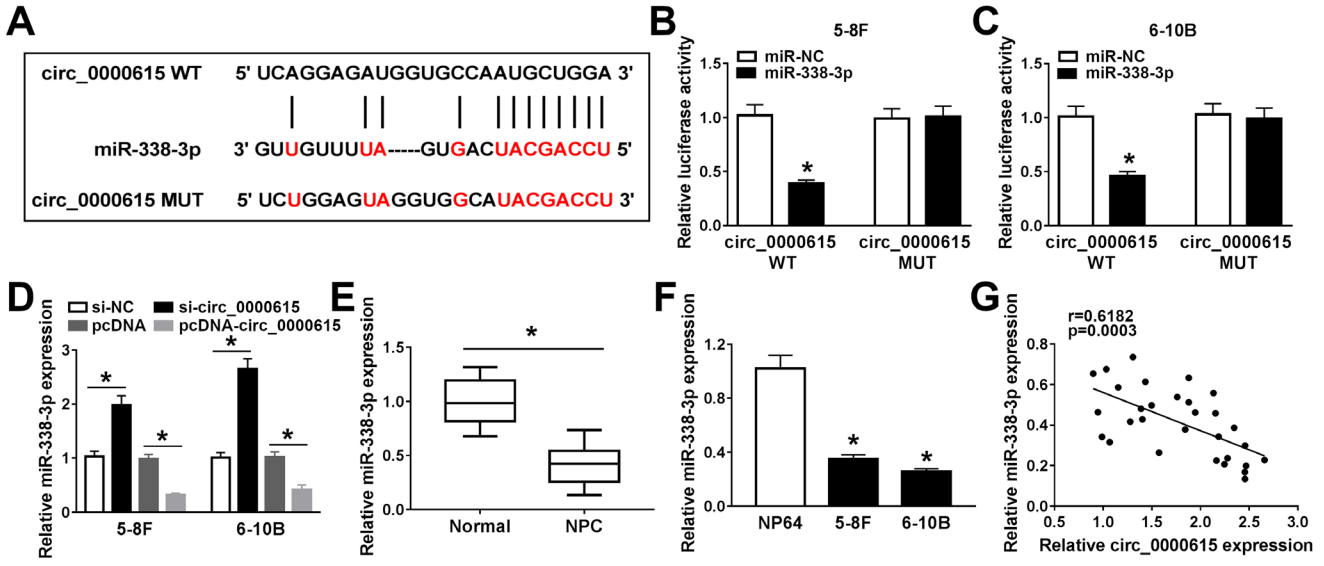

Figure 3. The interaction between circ_0000615 and miR-338-3p. A) The interaction between circ_0000615 and miR-338-3p was predicted by starBase v2.0. Mutated sites are shown in red color. B, C) The luciferase activity of 5–8F and 6–10B cells transfected with circ_0000615 WT or circ_0000615 MUT and miR-338-3p or miR-NC was determined. D) miR-338-3p expression was measured in 5–8F and 6–10B cells transfected with si-NC, circ_0000615, pcDNA, pcDNA-circ_0000615, respectively. E, F) miR-338-3p expression was examined in NPC and adjacent normal tissues (E) as well as NPC and normal cells (F). G) The relationship between circ_0000615 level and the miR-338-3p level was explored. *p<0.05

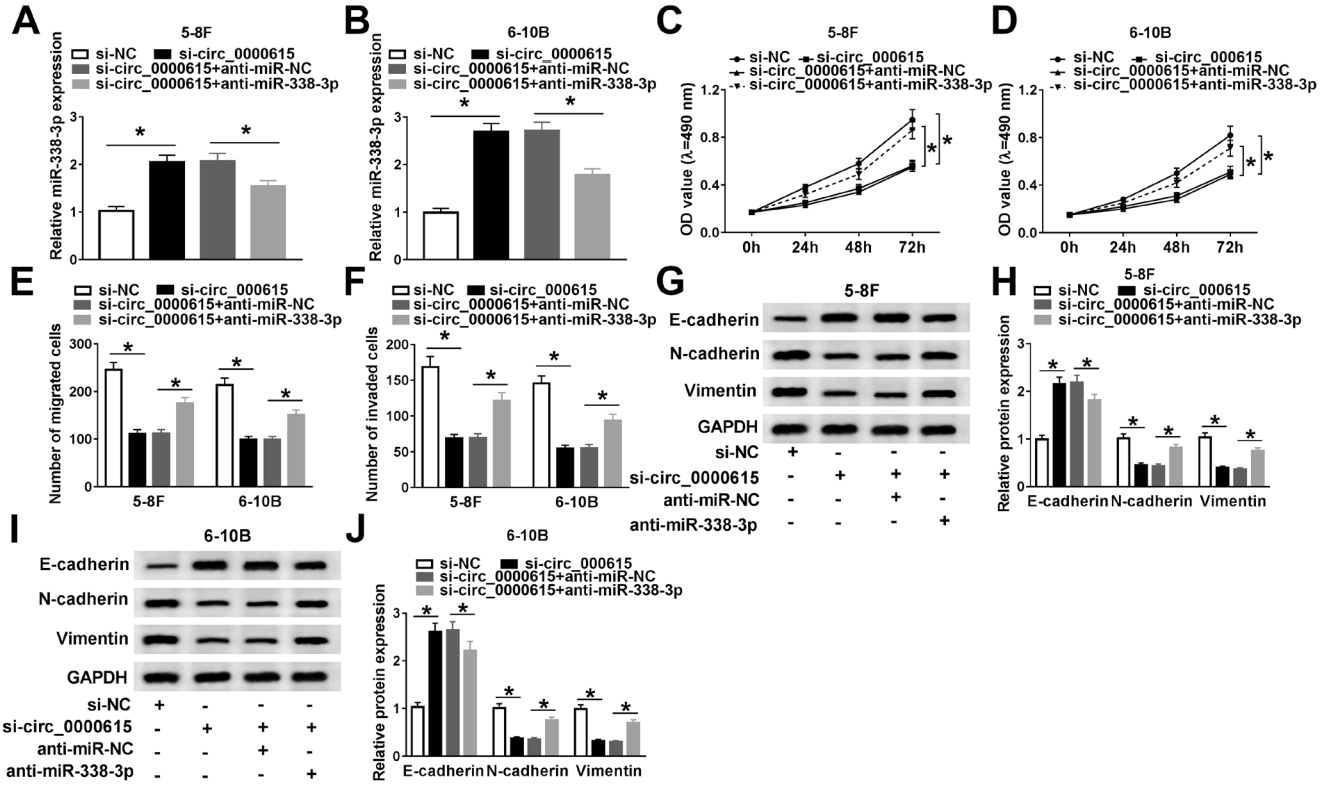

Figure 4. The effect of miR-338-3p knockdown on circ_0000615 depletion-regulated NPC cell progression. A, B) miR-338-3p expression was detected in 5–8F and 6–10B cells transfected with si-NC, si-circ_0000615, si-circ_0000615 + anti-miR-NC, or si-circ_0000615 + anti-miR-338-3p, respectively. C, D) Cell proliferation was assessed using the MTT assay. E, F) Cell migratory and invasive abilities were examined by the transwell assay. G–J) Western blot assay was employed to detect the levels of E-cadherin, N-cadherin, and Vimentin. *p<0.05

assay to verify this interaction. As demonstrated in Figures 5B and 5C, the luciferase activity of FGF2 3'-UTR-WT, but not FGF2 3'-UTR-MUT, was remarkably reduced by the overexpression of miR-338-3p. These results revealed that miR-338-3p targeted FGF2. Then, we analyzed the level of FGF2 in NPC tissues and found that FGF2 level was higher in NPC tissues than that in adjacent normal tissues (Figures 5D, 5E). Moreover, increased FGF2 level was observed in NPC cells (Figures 5F, 5G). Besides, we also confirmed that the FGF2 level was negatively correlated with the miR-338-3p level in NPC tissues (Figure 5H). On the other hand, the effect of miR-338-3p on FGF2 expression was investigated. The results demonstrated that FGF2 expression was upregulated by miR-338-3p knockdown and downregulated by miR-338-3p overexpression (Figures 5I–5K). Therefore, miR-338-3p suppressed FGF2 expression through interaction.

Furthermore, our data suggested that there was a positive correlation between the FGF2 level and circ_0000615 level (Figure 5L). Then, the linear regulatory relationship between the circ_0000615, miR-338-3p, and FGF2 was explored. As shown in Figures 5M–5O, FGF2 level was dramatically downregulated by circ_0000615 knockdown, and then partly rescued due to miR-338-3p depletion. Thus, circ_0000615 upregulated the level of FGF2 by inhibiting miR-338-3p expression.

FGF2 overexpression weakened the effect of circ_0000615 depletion on the growth of NPC cells. Next, we analyzed the role of FGF2 in circ_0000615-regulated cell

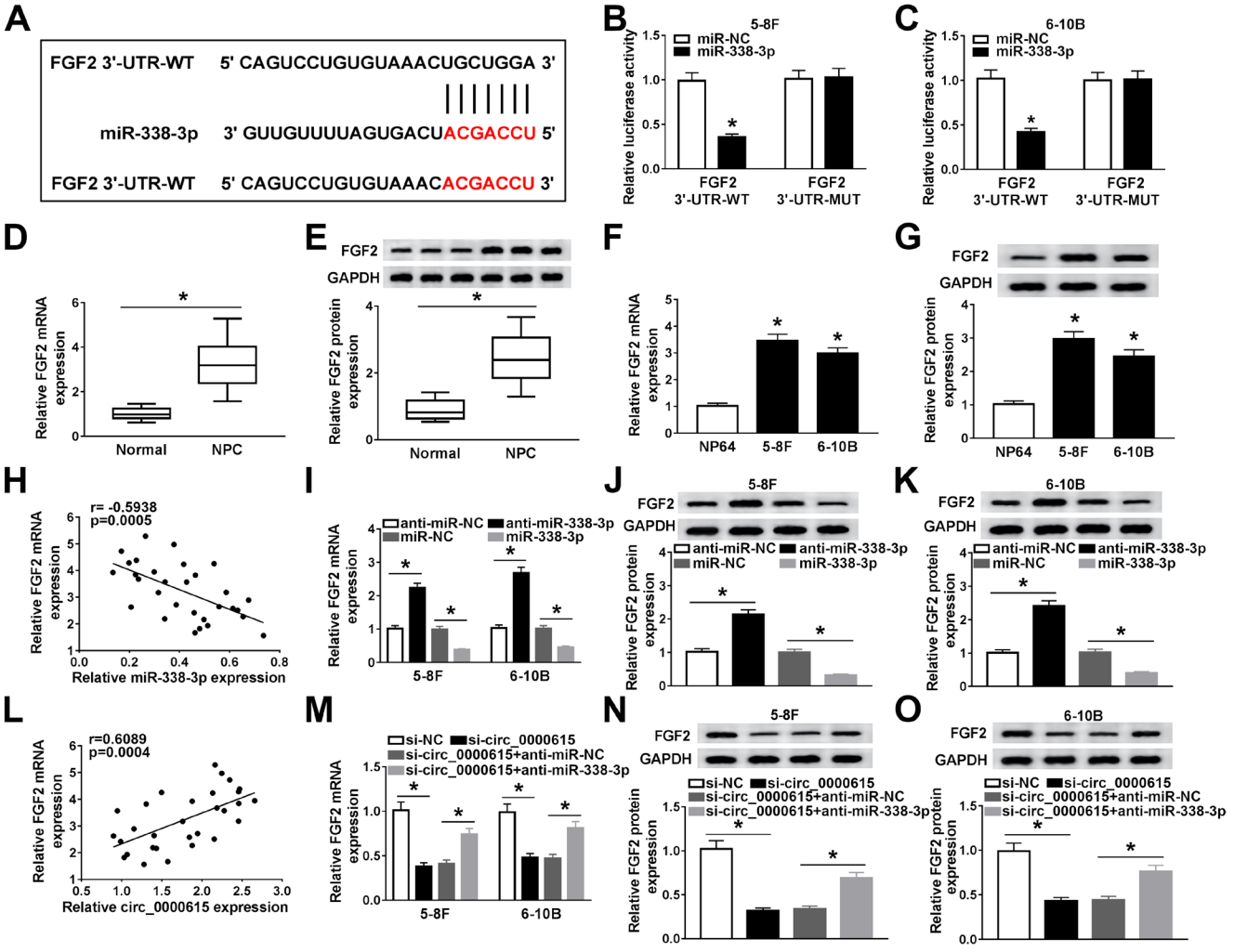

Figure 5. The interaction between miR-338-3p and FGF2. A) The interaction between miR-338-3p and FGF2 was predicted by starBase v2.0. Mutated sites were expressed as the red color. B, C) The luciferase activity was analyzed in 5–8F and 6–10B cells transfected with FGF2 3'-UTR-WT or FGF2 3'-UTR-MUT and miR-338-3p or miR-NC. D–G) The mRNA level and protein level of FGF2 were measured in NPC and adjacent normal tissues (D, E) as well as NPC and normal cells (F, G). H) The relationship between miR-338-3p level and FGF2 level was investigated. I–K) The mRNA level and protein level of FGF2 were detected in 5–8F and 6–10B cells transfected with anti-miR-NC, anti-miR-338-3p, miR-NC, or miR-338-3p, respectively. L) The relationship between the FGF2 level and circ_0000615 level was investigated. M–O) FGF2 expression was examined in 5–8F and 6–10B cells transfected with si-NC, si-circ_0000615, si-circ_0000615 + anti-miR-NC, or si-circ_0000615 + anti-miR-338-3p, respectively. *p<0.05

progression through transfecting si-NC, si-circ_0000615, si-circ_0000615 + pcDNA, or si-circ_0000615 + pcDNA-FGF2 into 5–8F and 6–10B cells. Then, the qRT-PCR assay and western blot assay were performed to detect the level of FGF2. The results indicated that the FGF2 level was downregulated by circ_0000615 knockdown and then upregulated due to FGF2 overexpression (Figures 6A–6C). Subsequently, the MTT assay was employed to detect cell proliferation ability. As shown in Figures 6D and 6E, circ_0000615 knockdown suppressed cell proliferation, whereas this effect was reversed by FGF2 overexpression. Furthermore, circ_0000615 knockdown-inhibited cell migration and invasion were promoted by FGF2 overexpression in 5–8F and 6–10B cells Figures 6F and 6G. Besides, we determined the levels of EMT markers and found that the effect of circ_0000615 knockdown on the levels of EMT markers was impaired by FGF2 overexpression (Figures 6H–6K). These results revealed that circ_0000615 regulated NPC cell progression by modulation of FGF2 expression.

Circ_0000615 depletion repressed tumor growth *in vivo*. To investigate the effect of circ_0000615 on tumor growth *in vivo*, 6 weeks old female SCID mice were subcutaneously injected with 5–8F cells transfected with circ_0000615 or sh-NC. After 7 days, tumor volume was measured every 4 days. As shown in Figure 7A, tumor volume was smaller in the sh-circ_0000615 group compared with that in the sh-NC group. Similarly, circ_0000615 knockdown reduced tumor weight (Figure 7B). Next, the levels of circ_0000615, miR-338-3p, and FGF2 in the sh-NC group and sh-circ_0000615 group were detected. As expected, circ_0000615 level (Figure 7C) and FGF2 level (Figures 7E, 7F) were downregulated as well as the miR-338-3p level (Figure 7D) was upregulated in the sh-circ_0000615 group. Therefore, circ_0000615 depletion suppressed tumor growth *in vivo*.

Discussion

NPC, with high metastasis, is cancer that is generally diagnosed at an advanced stage [25]. CircRNAs are related to the development of human cancers [26]. Lots of studies suggested that circRNAs played a pivotal function by regulating the levels of downstream genes in NPC cells. For example, Shuai et al. revealed that circRNA_0000285

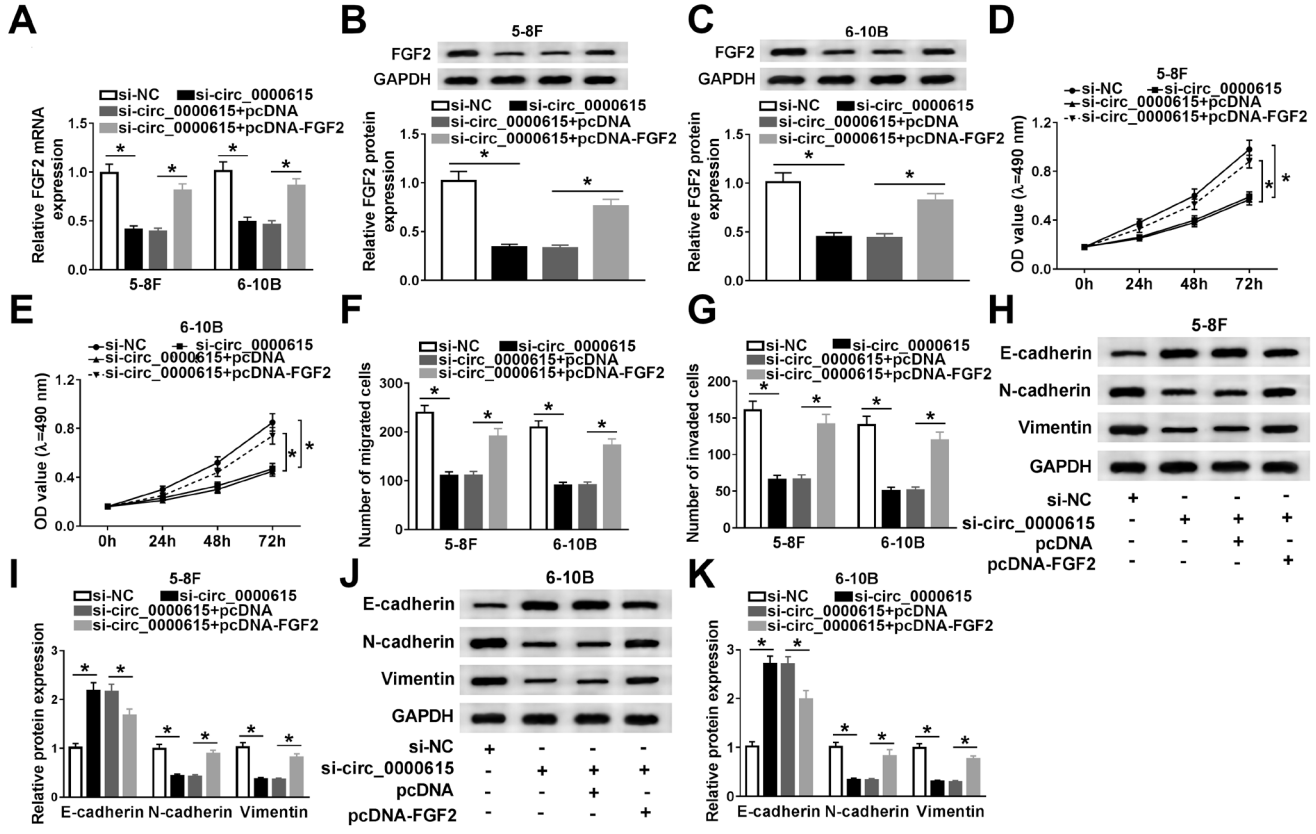

Figure 6. The effect of FGF2 overexpression on circ_0000615 depletion-regulated NPC cell progression. A–C) FGF2 expression was determined in 5–8F and 6–10B cells transfected with si-NC, si-circ_0000615, si-circ_0000615 + pcDNA, or si-circ_0000615 + pcDNA-FGF2, respectively. D, E) The MTT assay was employed to analyze cell proliferation ability. F, G) The transwell assay was conducted to investigate cell migratory and invasive abilities. H–K) The levels of E-cadherin, N-cadherin, and Vimentin were detected by western blot assay. *p<0.05

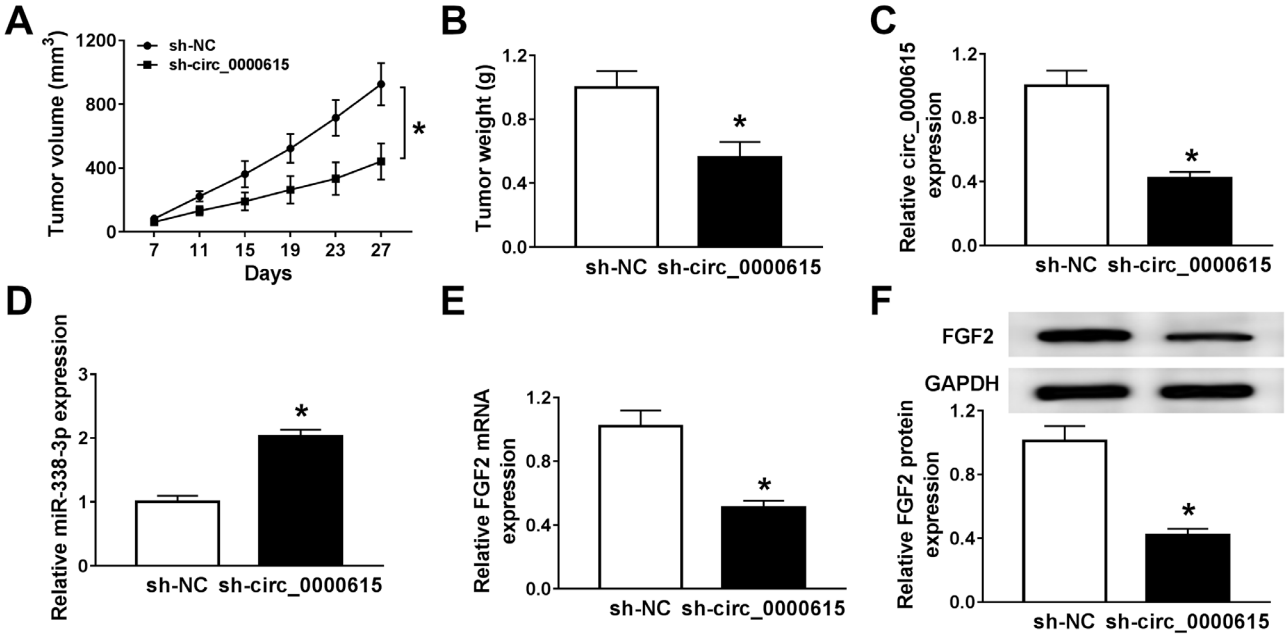

Figure 7. The effect of circ_0000615 depletion on tumor growth *in vivo*. A, B) Tumor volume (A) and tumor weight (B) were calculated in the sh-circ_0000615 group and the sh-NC group. C–E) The levels of circ_0000615, miR-338-3p, and FGF2 were detected by the qRT-PCR assay. F) The protein level of FGF2 was determined by western blot assay. *p<0.05

was considered as a biomarker for the prognosis of NPC and related to radiosensitivity [27]. Chen et al. confirmed that circRNA_000543 was highly expressed in NPC tissues and modulated cell growth via regulating miR-9 level [28]. Wei et al. indicated that circ_0008450 overexpression accelerated NPC cell growth as well as invasion through binding to miR-577 [29]. Hence, the analysis of circRNA in NPC cells is essential.

Circ_0000615, also known as circRNA-ZNF609, was reported to serve as an oncogene in various cancers, such as rhabdomyosarcoma [30], colorectal cancer [31], renal carcinoma [32], and breast cancer [33]. Furthermore, Zhu et al. confirmed that circ_0000615 was highly expressed in NPC tissues, and circ_0000615 depletion suppressed the proliferation and mobility of NPC cells [11]. Consistent with these data, our results suggested that the circ_0000615 level was upregulated in NPC tissues and cells, and circ_0000615 downregulation repressed the proliferation, mobility, and EMT of NPC cells. These data revealed that circ_0000615 acted as a positive regulator in NPC development.

Amounting studies demonstrate that circRNA mediates the level of miRNA to affect cell progression by targeting miRNA [34]. For instance, circular RNA_000926 repressed miR-411 expression via targeting miR-411 in renal cell carcinoma [35]. Next, we used an online tool starBase v2.0 to explore the downstream genes of circ_0000615. The results indicated that miR-338-3p was a potential target of circ_0000615. Subsequently, the interaction between circ_0000615 and miR-338-3p was confirmed by the dual-luciferase reporter assay. Furthermore, our results revealed that circ_0000615 negatively regulated the level of miR-338-3p in NPC cells. miR-338-3p, a tumor suppressor, has been uncovered to inhibit cell proliferation and mobility in many human cancers, including breast cancer [36], renal cell carcinoma [37], hepatocellular carcinoma [38], and glioma [39]. In NPC, the miR-338-3p level was upregulated, and miR-338-3p repressed NPC cell proliferation and mobility [18]. These data were in agreement with our results. Then, we speculated that circ_0000615 regulated the growth of NPC cells through modulating miR-338-3p expression. Subsequently, a series of experiments were carried out to verify this hypothesis. The result was accordant with our hypothesis, circ_0000615 inhibited miR-338-3p expression to modulate the growth of NPC cells.

It is widely accepted that miRNA acts as a sponge for mRNA via targeting 3'-untranslated region (UTR) of target mRNA [40]. To further explore the molecular mechanism of miR-338-3p, an online tool starBase v2.0 was employed to predict the potential targets of miR-338-3p. The results suggested that miR-338-3p likely bound to FGF2. Then, this interaction was verified by the dual-luciferase reporter assay. Moreover, the FGF2 level was downregulated by miR-338-3p. FGF2, considered as an oncogene, was highly expressed in various cancers, including thyroid cancer [41], endometrial carcinoma [42], and NPC [21]. Consistent with these data, our results suggested that the FGF2 level was increased in NPC tissues and cells.Furthermore, we found that circ_0000615 repressed miR-338-3p expression

to upregulate the FGF2 level, meaning that circ_0000615 exerted function through regulating the FGF2 level. Then, the effect of FGF2 on circ_0000615-regulated cell progression was explored. As expected, FGF2 knockdown reversed the effect of circ_0000615 on NPC cell progression. Taken together, circ_0000615 regulated the growth of NPC cells via modulating miR-338-3p/FGF2 axis. In general, circRNA, as an oncogene, promoted tumor growth *in vivo* [43]. Then, we analyzed the effect of circ_0000615 on tumor growth. As expected, tumor volume and weight were downregulated by circ_0000615 depletion. Thus, circ_0000615 depletion inhibited tumor growth of NPC *in vivo*.

In conclusion, our data demonstrated that circ_0000615 knockdown suppressed the growth and mobility of NPC cells through modulating miR-338-3p/FGF2 axis. Our findings provided a potential target for the therapy of NPC patients.

Acknowledgments: This study was supported by the Medical Scientific Research Foundation of Guangdong Province of China (Grant No. B2018064).

References

[1] CHO WC. Nasopharyngeal carcinoma: molecular biomarker discovery and progress. Mol Cancer 2007; 6: 1. https://doi.org/10.1186/1476-4598-6-1

[2] CAO SM, SIMONS MJ, QIAN CN. The prevalence and prevention of nasopharyngeal carcinoma in China. Chin J Cancer 2011; 30: 114–119. https://doi.org/10.5732/cjc.010.10377

[3] LAI SZ, LI WF, CHEN L, LUO W, CHEN YY et al. How does intensity-modulated radiotherapy versus conventional two-dimensional radiotherapy influence the treatment results in nasopharyngeal carcinoma patients? Int J Radiat Oncol Biol Phys 2011; 80: 661–668. https://doi.org/10.1016/j.ijrobp.2010.03.024

[4] HILDESHEIM A, WANG CP. Genetic predisposition factors and nasopharyngeal carcinoma risk: a review of epidemiological association studies, 2000–2011: Rosetta Stone for NPC: genetics, viral infection, and other environmental factors. Semin Cancer Biol 2012; 22: 107–116. https://doi.org/10.1016/j.semcancer.2012.01.007

[5] HUANG L, HU C, CHAO H, ZHANG Y, LI Y et al. Drug-resistant endothelial cells facilitate progression, EMT and chemoresistance in nasopharyngeal carcinoma via exosomes. Cell Signal 2019; 63: 109385. https://doi.org/10.1016/j.cellsig.2019.109385

[6] WANG JY, LU AQ, CHEN LJ. LncRNAs in ovarian cancer. Clin Chim Acta 2019; 490: 17–27. https://doi.org/10.1016/j.cca.2018.12.013

[7] BARTEL DP. MicroRNAs: genomics, biogenesis, mechanism, and function. Cell 2004; 116: 281–297. https://doi.org/10.1016/s0092-8674(04)00045-5

[8] MEMCZAK S, JENS M, ELEFSINIOTI A, TORTI F, KRUEGER J et al. Circular RNAs are a large class of animal RNAs with regulatory potency. Nature 2013; 495: 333–338. https://doi.org/10.1038/nature11928

[9] WANG J, LI H. CircRNA circ_0067934 silencing inhibits the proliferation, migration and invasion of NSCLC cells and correlates with unfavorable prognosis in NSCLC. Eur Rev Med Pharmacol Sci 2018; 22: 3053–3060. https://doi.org/10.26355/eurrev_201805_15063

[10] ZHANG X, WANG S, WANG H, CAO J, HUANG X et al. Circular RNA circNRIP1 acts as a microRNA-149-5p sponge to promote gastric cancer progression via the AKT1/mTOR pathway. Mol Cancer 2019; 18: 20. https://doi.org/10.1186/s12943-018-0935-5

[11] ZHU L, LIU Y, YANG Y, MAO XM, YIN ZD. CircRNA ZNF609 promotes growth and metastasis of nasopharyngeal carcinoma by competing with microRNA-150-5p. Eur Rev Med Pharmacol Sci 2019; 23: 2817–2826. https://doi.org/10.26355/eurrev_201904_17558

[12] MULLANY LE, HERRICK JS, WOLFF RK, SLATTERY ML. MicroRNA seed region length impact on target messenger RNA expression and survival in colorectal cancer. PLoS One 2016; 11: e0154177. https://doi.org/10.1371/journal.pone.0154177

[13] WANG S, LI Q, WANG K, DAI Y, YANG J et al. Decreased expression of microRNA-31 associates with aggressive tumor progression and poor prognosis in patients with bladder cancer. Clin Transl Oncol 2013; 15: 849–854. https://doi.org/10.1007/s12094-013-1014-4

[14] XU B, LIU J, XIANG X, LIU S, ZHONG P et al. Expression of miRNA-143 in pancreatic cancer and its clinical significance. Cancer Biother Radiopharm 2018; 33: 373–379. https://doi.org/10.1089/cbr.2018.2500

[15] ELGHOROURY EA, ELDINE HG, KAMEL SA, ABDEL-RAHMAN AH, MOHAMMED A et al. Evaluation of miRNA-21 and miRNA Let-7 as prognostic markers in patients with breast cancer. Clin Breast Cancer 2018; 18: e721–e726. https://doi.org/10.1016/j.clbc.2017.11.022

[16] ZHAO J, CHEN Y, LIU F, YIN M. Overexpression of miRNA-143 inhibits colon cancer cell proliferation by inhibiting glucose uptake. Arch Med Res 2018; 49: 497–503. https://doi.org/10.1016/j.arcmed.2018.12.009

[17] ZHOU X, ZHENG J, TANG Y, LIN Y, WANG L et al. EBV encoded miRNA BART8-3p promotes radioresistance in nasopharyngeal carcinoma by regulating ATM/ATR signaling pathway. Biosci Rep 2019; 39. https://doi.org/10.1042/bsr20190415

[18] SHAN Y, LI X, YOU B, SHI S, ZHANG Q et al. MicroRNA-338 inhibits migration and proliferation by targeting hypoxia-induced factor 1alpha in nasopharyngeal carcinoma. Oncol Rep 2015; 34: 1943–1952. https://doi.org/10.3892/or.2015.4195

[19] BEENKEN A, MOHAMMADI M. The FGF family: biology, pathophysiology and therapy. Nat Rev Drug Discov 2009; 8: 235–253. https://doi.org/10.1038/nrd2792

[20] KORC M, FRIESEL RE. The role of fibroblast growth factors in tumor growth. Curr Cancer Drug Targets 2009; 9: 639–651. https://doi.org/10.2174/156800909789057006

[21] DE MOERLOOZE L, SPENCER-DENE B, REVEST JM, HAJIHOSSEINI M, ROSEWELL I et al. An important role for the IIIb isoform of fibroblast growth factor receptor 2 (FGFR2) in mesenchymal-epithelial signalling during mouse organogenesis. Development 2000; 127: 483–492.

[22] XU M, TIAN GL, HAO CC, SHI M, ZHA DJ et al. MicroRNA-29 targets FGF2 and inhibits the proliferation, migration and invasion of nasopharyngeal carcinoma cells via PI3K/AKT signaling pathway. Eur Rev Med Pharmacol Sci 2019; 23: 5215–5222. https://doi.org/10.26355/eurrev_201906_18186

[23] SUN Y, ZHANG T, WANG C, JIN X, JIA C et al. MiRNA-615-5p functions as a tumor suppressor in pancreatic ductal adenocarcinoma by targeting AKT2. PLoS One 2015; 10: e0119783. https://doi.org/10.1371/journal.pone.0119783

[24] ANASTASIADOU E, JACOB LS, SLACK FJ. Non-coding RNA networks in cancer. Nat Rev Cancer 2018; 18: 5–18. https://doi.org/10.1038/nrc.2017.99

[25] ZHOU TJ, ZHANG SL, HE CY, ZHUANG QY, HAN PY et al. Downregulation of mitochondrial cyclooxygenase-2 inhibits the stemness of nasopharyngeal carcinoma by decreasing the activity of dynamin-related protein 1. Theranostics 2017; 7: 1389–1406. https://doi.org/10.7150/thno.17647

[26] MENG S, ZHOU H, FENG Z, XU Z, TANG Y et al. CircRNA: functions and properties of a novel potential biomarker for cancer. Mol Cancer 2017; 16: 94. https://doi.org/10.1186/s12943-017-0663-2

[27] SHUAI M, HONG J, HUANG D, ZHANG X, TIAN Y. Upregulation of circRNA_0000285 serves as a prognostic biomarker for nasopharyngeal carcinoma and is involved in radiosensitivity. Oncol Lett 2018; 16: 6495–6501. https://doi.org/10.3892/ol.2018.9471

[28] CHEN L, ZHOU H, GUAN Z. CircRNA_000543 knockdown sensitizes nasopharyngeal carcinoma to irradiation by targeting miR-9/platelet-derived growth factor receptor B axis. Biochem Biophys Res Commun 2019; 512: 786–792. https://doi.org/10.1016/j.bbrc.2019.03.126

[29] WEI H, LIU D, SUN J, MAO Y, ZHAO L et al. Circular RNA circ_0008450 upregulates CXCL9 expression by targeting miR-577 to regulate cell proliferation and invasion in nasopharyngeal carcinoma. Exp Mol Pathol 2019; 110: 104288. https://doi.org/10.1016/j.yexmp.2019.104288

[30] ROSSI F, LEGNINI I, MEGIORNI F, COLANTONI A, SANTINI T et al. Circ-ZNF609 regulates G1-S progression in rhabdomyosarcoma. Oncogene 2019; 38: 3843–3854. https://doi.org/10.1038/s41388-019-0699-4

[31] WU L, XIA J, YANG J, SHI Y, XIA H et al. Circ-ZNF609 promotes migration of colorectal cancer by inhibiting Gli1 expression via microRNA-150. J BUON 2018; 23: 1343–1349.

[32] XIONG Y, ZHANG J, SONG C. CircRNA ZNF609 functions as a competitive endogenous RNA to regulate FOXP4 expression by sponging miR-138-5p in renal carcinoma. J Cell Physiol 2019; 234: 10646–10654. https://doi.org/10.1002/jcp.27744

[33] WANG S, XUE X, WANG R, LI X, LI Q et al. CircZNF609 promotes breast cancer cell growth, migration, and invasion by elevating p70S6K1 via sponging miR-145-5p. Cancer Manag Res 2018; 10: 3881–3890. https://doi.org/10.2147/cmar.s174778

[34] XIONG DD, FENG ZB, LAI ZF, QIN Y, LIU LM et al. High throughput circRNA sequencing analysis reveals novel insights into the mechanism of nitidine chloride against hepatocellular carcinoma. Cell Death Dis 2019; 10: 658. https://doi.org/10.1038/s41419-019-1890-9

[35] ZHANG D, YANG XJ, LUO QD, FU DL, LI ZL et al. Downregulation of circular RNA_000926 attenuates renal cell carcinoma progression through miRNA-411-dependent CDH2 inhibition. Am J Pathol 2019. https://doi.org/10.1016/j.ajpath.2019.06.016

[36] ZHANG L, DING F. Hsa_circ_0008945 promoted breast cancer progression by targeting miR-338-3p. Onco Targets Ther 2019; 12: 6577–6589. https://doi.org/10.2147/ott.s213994

[37] ZHANG X, WANG C, LI H, NIU X, LIU X et al. miR-338-3p inhibits the invasion of renal cell carcinoma by downregulation of ALK5. Oncotarget 2017; 8: 64106–64113. https://doi.org/10.18632/oncotarget.19329

[38] JI D, HU G, ZHANG X, YU T, YANG J. Long non-coding RNA DSCAM-AS1 accelerates the progression of hepatocellular carcinoma via sponging miR-338-3p. Am J Transl Res 2019; 11: 4290–4302. PMID: 31396335

[39] LIU X, ZHU Q, GUO Y, XIAO Z, HU L et al. LncRNA LINC00689 promotes the growth, metastasis and glycolysis of glioma cells by targeting miR-338-3p/PKM2 axis. Biomed Pharmacother 2019; 117: 109069. https://doi.org/10.1016/j.biopha.2019.109069

[40] WANG D, XIN L, LIN JH, LIAO Z, JI JT et al. Identifying miRNA-mRNA regulation network of chronic pancreatitis based on the significant functional expression. Medicine (Baltimore) 2017; 96: e6668. https://doi.org/10.1097/md.0000000000006668

[41] HUANG JK, MA L. LncRNA-MALAT1 promotes angiogenesis of thyroid cancer by modulating tumor-associated macrophage FGF2 protein secretion. J Cell Biochem 2017; 118: 4821–4830. https://doi.org/10.1002/jcb.26153

[42] CHEN P, XING T, WANG Q, LIU A, LIU H et al. MicroRNA-202 inhibits cell migration and invasion through targeting FGF2 and inactivating Wnt/beta-catenin signaling in endometrial carcinoma. Biosci Rep 2019. https://doi.org/10.1042/bsr20190680

[43] REN S, LIU J, FENG Y, LI Z, HE L et al. Knockdown of circDENND4C inhibits glycolysis, migration and invasion by up-regulating miR-200b/c in breast cancer under hypoxia. J Exp Clin Cancer Res 2019; 38: 388. https://doi.org/10.1186/s13046-019-1398-2